NANO LETTERS

pubs.acs.org/NanoLett

Resistive Switching Multistate Nonvolatile Memory Effects in a Single Cobalt Oxide Nanowire

Kazuki Nagashima,[†] Takeshi Yanagida,*[,†,‡] Keisuke Oka,[†] Masateru Taniguchi,[†,‡] Tomoji Kawai,*[,†,§] Jin-Soo Kim,[§] and Bae Ho Park[§]

[†]Institute of Scientific and Industrial Research, Osaka University, 8-1 Mihogaoka, Ibaraki, Osaka 567-0047, Japan, [‡]PRESTO, Japan Science and Technology Agency, 4-1-8 Honcho, Kawaguchi, Saitama 332-0012, Japan, and [§]Department of Physics, Division of Quantum Phases & Devices, Konkuk University, Seoul 143-701, Republic of Korea

ABSTRACT A multistate nonvolatile memory operated at sublithographic scale has been strongly desired since other nonvolatile memories have confronted the fundamental size limits owing to their working principles. Resistive switching (RS) in metal−oxide−metal junctions, so-called ReRAM, is promising for next generation high-density nonvolatile memory. Self-assembled oxide nanowire-based RS offers an attractive solution not only to reduce the device size beyond the limitation of current lithographic length scales but also to extract the underlying nanoscale RS mechanisms. Here we demonstrate the multistate bipolar RS of a single Co_3O_4 nanowire (10 nm scale) with the endurance up to 10^8. In addition, we succeeded to extract a voltage-induced nanoscale RS mechanism rather than current-induced RS. These findings would open up opportunities to explore not only for the intrinsic nanoscale RS mechanisms with the ultimate size limit but also for next generation multistate three-dimensional ReRAM.

KEYWORDS Resistive switching, nonvolatile memory, nanowires, cobalt oxides, multistate memory

Resistive switching (RS) phenomena in metal−oxide−metal sandwich junctions, so-called "ReRAM" and/or "Memristors", have attracted a great deal of scientific and industrial interest as next-generation high-density nonvolatile memories due to their structural simplicity and excellent memory characteristics compared with existing nonvolatile memories such as flash-memory, FeRAM, MRAM and PRAM.[1−5] Previously various oxides including NiO,[6−10,22,23] TiO_2,[11−14] CuO,[15] CoO[16,17] and others[18−21] have been investigated. The observed RS behaviors have been categorized into three types including bipolar,[9,13,14,17,19−21,23] unipolar,[6−8,11,12,15,16,18,22] and threshold switching.[10] Although several models have been proposed to explain RS, a model based on nanoscale conducting filaments within insulators has most successfully explained many RS features.[6,7,9−20] However, the mechanisms especially at nanoscale are under debate due to the finite size of such conducting filaments.[19,20] To achieve high-density memory, it is crucial to reduce the size of RS cells beyond the limitation of current lithographic length scales. ReRAM has been especially expected to show the multistate memory effects at sublithographic scale, hardly attainable with other nonvolatile memories due to their working principles. Thus the scaling down of RS cells is strongly desired not only for understanding the underlying RS mechanisms at sublithographic scale but also for improving the characteristics. Although the bottom-up approach[24] using self-assembled oxide nanowires is a promising solution for scaling down the device size, the reliable multistate RS of oxide nanowire had been unfeasible.[22,23] In this Letter, we demonstrate for the first time the multistate bipolar RS effect of a single cobalt oxide (p-type) nanowire (10 nm scale) with endurance up to 10^8.

Cobalt oxide nanowires were fabricated as core-MgO/shell-cobalt oxide nanowires by an in situ nanowire template method.[23,25−27] MgO nanowires were grown on MgO (100) single crystal substrate by Au catalyst assisted vapor−liquid−solid (VLS) growth using pulsed laser deposition. The details of MgO nanowire growth can be seen elsewhere[28−34] (see Supporting Information). The typical growth conditions were 750 °C of the substrate temperature and 10 Pa ($Ar:O_2$ = 1000:1) of ambient pressure. The length and the diameter of fabricated MgO nanowires were typically 5 μm and 10 nm, respectively. A cobalt oxide layer was deposited onto the core nanowires without atmospheric exposure. A Co_3O_4 pellet (99.9% pure) was used as a target. Prior to the shell layer formation, the chamber pressure was set to be less than 5×10^{-6} Pa, and then Ar gas (99.9999% pure) was introduced. The shell layer formation was performed under room temperature (RT) and 10^{-1} Pa of the ambient pressure. The microstructures, compositions, and crystallinity of core−shell nanowires were evaluated by field emission scanning electron microscopy (FESEM) and high-resolution transmission electron microscopy (HRTEM) equipped with energy dispersed electron spectroscopy (EDS). To evaluate the transport properties of MgO/cobalt oxide nanowires, we

*To whom correspondence should be addressed: e-mail, yanagi32@sanken.osaka-u.ac.jp; tel, +81-6-6879-4294; fax, +81-6-6875-2440. E-mail: kawai@sanken.osaka-u.ac.jp.

Received for review: 12/30/2009
Published on Web: 03/12/2010

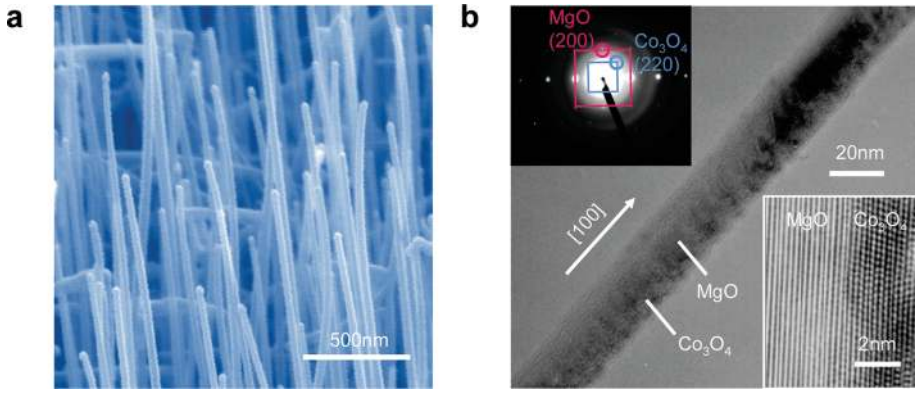

FIGURE 1. (a) FESEM (false color) and (b) HRTEM images of the MgO/Co_3O_4 heterostructured nanowires. Upper left and lower right insets in (b) show the selected area electron diffraction (SAED) pattern and the magnified heterointerface of nanowires, respectively.

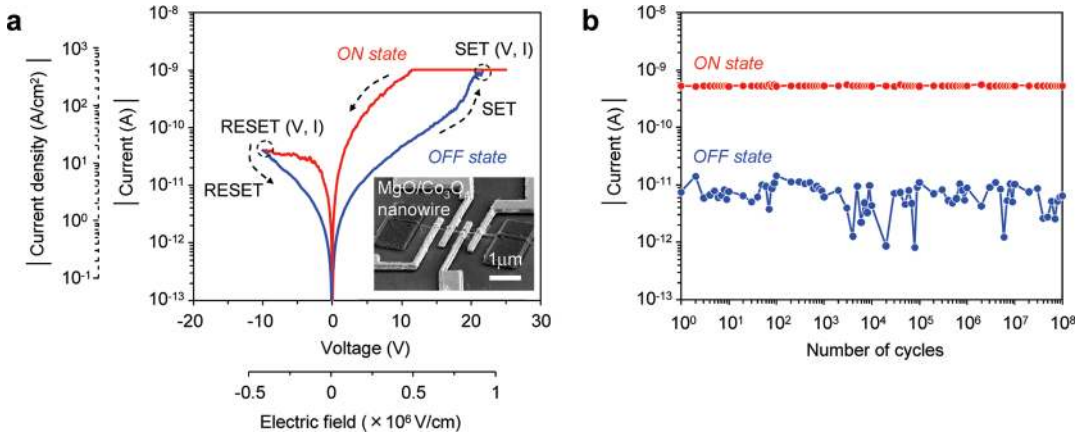

FIGURE 2. (a) Typical $I-V$ characteristics of the individual MgO/Co_3O_4 nanowire device. The external scales show the corresponding current density (y axis) and electric field (x axis), respectively. The inset shows the FESEM image of the nanowire device structure. All $I-V$ characteristics were measured by using adjacent two electrodes. A typical nanogap distance was ~250 nm. (b) Switching endurance data of the MgO/Co_3O_4 nanowire device. For switching endurance, the applied SET (from HRS to LRS) voltage, the RESET (from LRS to HRS) voltage, and the compliance current were 15 V (500 μs), -3 V (200 μs), and 10^{-7} A, respectively. Resistances of both LRS and HRS were read at 2 V.

utilized the devices composed of individual nanowires, which were fabricated on degenerately doped n-type silicon substrate capped with thermally oxidized SiO_2 layer with 300 nm of the thickness.[35,36] Combining photolithography and electron beam (EB) lithography processes enables electrode patterns to be defined on the SiO_2/Si substrate, followed by metal deposition of Pt/Au (20/100 nm). The transport measurements were performed in atmospheric air at RT by using semiconductor parameter analyzer (Keithley 4200SCS).

Figure 1a shows the FESEM image of MgO (core)/cobalt oxide (shell) nanowires grown on the substrate. Most nanowires are grown vertically to the substrate due to the preferential crystal growth along the MgO (100) direction.[28−34] The diameter, the crystal structure, and the composition of core/shell nanowires were evaluated by HRTEM-EDS, as shown in Figure 1b (see part 1 in Supporting Information). The uniformity of the shell layer with the grainlike morphology can be seen. The diameter of MgO nanowire was typically 10 nm and the shell thickness was 5 nm, which is controllable by varying the deposition time. The EDS and ED pattern analysis identified that the crystal structure of shell layer is a spinel Co_3O_4 (see part 1 in Supporting Information). Figure 2a shows the current−voltage ($I-V$) characteristics of the nanowire device in a semilogarithmic current scale. The inset shows the FESEM image of the device. Initially the nanowire was highly insulative (10^{13} Ω at 1 V). By performing a so-called "*forming*" process with high electric field,[14,15,18,21] the resistance decreased down to 10^{10} Ω (see part 2 of the Supporting Information). After the forming process, the $I-V$ data of Figure 2a were obtained with the compliance current of 10^{-9} A. The presence of bipolar RS, which is defined as a polarity-dependent RS,[8,9,13,14,17,19−21] can be clearly seen. When a positive voltage was applied, a "SET" process from a high resistance OFF state (HRS) to a low resistance ON state (LRS) appeared, whereas applying the negative voltage resulted in a "RESET" process from LRS to HRS. Once the SET or RESET process was performed, LRS and HRS were kept as long as the electric field was applied to the same polarity. The occurrence of such a bipolar RS within the shell layer was confirmed by performing the $I-V$ measurement for the device comprised of only the MgO core nanowire,

DOI: 10.1021/nl9042906 | *Nano Lett.* **2010,** *10,* 1359--1363

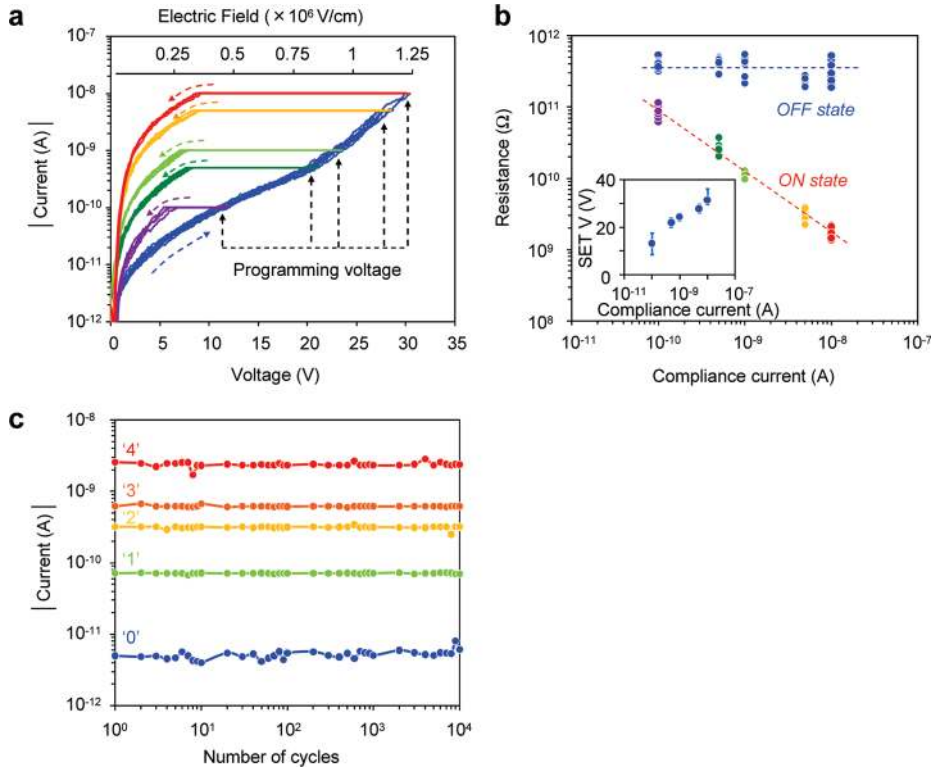

FIGURE 3. (a) $I-V$ characteristics of the SET process when varying the compliance current ($10^{-10}-10^{-8}$ A). (b) Compliance current dependence of the nanowire resistance. Resistances were read at 5 V in both LRS and HRS. The same RESET voltage of −20 V was applied in each measurement. The inset shows the relationship between the compliance and the SET voltage. (c) Switching endurance data for various programming SET voltages (5, 10, 15, 20 V, 1 ms). RESET voltage was set to be −3 V (1 ms) in each experiment. Resistances for both LRS and HRS were read at 2 V.

where RS was not observed at all (see part 2 of the Supporting Information). Figure 2b shows the switching endurance of nanowire device. The switching endurance was confirmed at least 10^8 times, which exceeds the limitation of current flash memories. As to the retention time, both HRS and LRS were maintained in vacuum at least up to 10^4 s (see part 3 of the Supporting Information). Thus these results highlight the nonvolatile bipolar RS memory effects in the present nanowire device. The operating voltage (∼15−40 V) seems to be larger than typical values of thin film devices (∼1−5 V).[16,17] We calculated the electric field intensity (∼0.6−1.6 × 10^6 V/cm), which is comparable to that of thin film devices (∼(0.2−1) × 10^6 V/cm).[16,17] Thus the apparent discrepancy in the operating voltages between nanowire and thin film devices is due to the different gap distance between electrodes. The bipolar RS could be operated for the current range (∼10^{-9} A), which is much lower than typical operating currents (∼10^{-2} A) for the thin film devices.[17] Since the cross-sectional area of the Co_3O_4 shell layer is ∼10^{-4} μm^2, which is at least 6 orders of magnitude smaller than typical thin film devices previously reported, 10^2 μm^2,[17] the reduction of operating current level might be also related to the size effects of RS events. Although several models have been proposed for RS behavior,[6,10,11,14,19−21] a so-called filament model, which explains a RS in terms of the formation and rupture of conducting filaments within insulators, is a promising model. One of the unique features of the filament model is the presence of a *forming* process. As mentioned above, the present nanowire devices exhibited the *forming* process in the first $I-V$ sweep (see part 2 in the Supporting Information). On the basis of the filament model,[6,7,9−20] the LRS resistance is determined by the number and/or the size of nanoscale conducting filaments. Since the size of the filaments in present nanowire devices is confined to less than the size of nanowire, the confinement effects of conducting filaments within nanowires might result in a decrease of the current level for RS. Thus these results highlight the presence of nonvolatile bipolar RS memory effects within the present nanowire device down to a 10 nm size range, and the low power consumption properties.

Figure 3a shows the $I-V$ characteristics of SET processes when the compliance currents ranged from 10^{-10} to 10^{-8} A. For the RESET process, a constant voltage of −20 V was applied in each measurement. It can be seen that varying the compliance current value (i.e., programming voltage) resulted in the variation of LRS resistance, although the HRS resistance in each measurement was almost identical. More importantly, there was a systematic relationship between the compliance current and the LRS resistance, indicating the "multistate memory effects". Figure 3b shows the compliance current dependence on the resistances of both LRS and HRS. The resistance values of both LRS and HRS

DOI: 10.1021/nl9042906 | *Nano Lett.* **2010,** *10,* 1359--1363

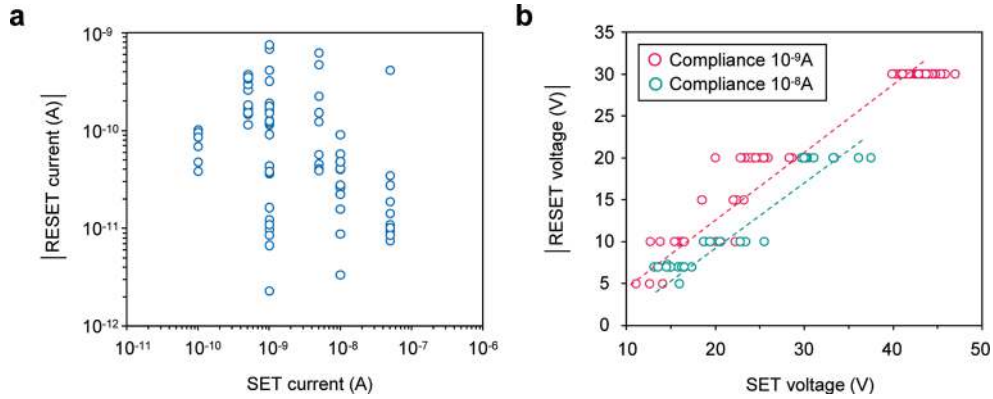

FIGURE 4. (a) Relationship between SET current and RESET current in RS. (b) Relationship between SET voltage and RESET voltage in RS. The data were obtained under a couple of compliance currents (10^{-9} and 10^{-8} A).

were measured at 5 V. LRS resistance systematically decreased with increasing the compliance current. The LRS/HRS resistance ratio increased from 3 to 300 when increasing the compliance current from 10^{-10} to 10^{-8} A. Recently Jung et al.[5] reported controllable three different resistance states by utilizing $Ge_2Sb_2Te_5$/GeTe core−shell heterostructured nanowires. The present oxide nanowire ReRAM devices can offer more multistate memory effects by just programming the compliance current in 10 nm size range. Figure 3c shows the endurance data when varying the programming voltage. The stable RS for each memory state can be seen up to 10^4 times. These results highlight the feasibility of oxide nanowire-based nonvolatile RS devices for high density and multistate memory.

Next we examine the mechanisms of bipolar RS with the multistate memory effects in the present nanowire devices. In the filament model,[6,7,9−20] the rupture and formation of filaments result in SET and RESET processes, respectively. The occurrence of both SET and RESET processes has been attributed to (1) Joule heating, (2) electrochemical redox events with filaments, and others.[6,8,11,12,17,19,20] The polarity dependence of bipolar RS seems to be consistent with the scenario based on an electrochemical redox.[8,17,19,20] Since Co_3O_4 is a p-type semiconductor,[37] the conducting path might be composed of oxygen-rich phases. The importance of anion and/or cation movements has been indicated for bipolar RS mechanisms,[8,17,19,20] and thus it would be very interesting to identify whether the bipolar RS in nanowire devices is induced by the electric field or the current.[19] To confirm this, we have investigated the relationship between RESET and SET voltage and/or currents. Figure 4 shows the relationships between RESET and SET voltages and/or currents. Here, SET voltage was defined as the voltage where the current reached to the compliance current (10^{-9} A). There is a reasonable correspondence between SET voltage and RESET voltage, whereas no clear relationship between SET current and RESET current exists, which completely differs from the trends of current-induced unipolar thin film devices (see part 4 in the Supporting Information). The relationships between the resistance and the voltage were also analyzed (see parts 5 in the Supporting Information). Thus these results highlight that the bipolar RS in present nanowire devices is induced by the electric field rather than the current, inferring the electrochemical redox events via the ion movements within nanowires. Further investigations, including real time composition variation analysis and/or atmosphere dependent transport measurements, should be undertaken to clarify the detailed redox based RS mechanisms.

In conclusion, we successfully demonstrate the sublithographic scale multistate bipolar RS in MgO/Co_3O_4 core/shell nanowires with endurance up to 10^8. A voltage-induced RS mechanism was identified by analyzing the RS properties. These findings would open up opportunities to explore not only for the intrinsic nanoscale RS mechanisms with the ultimate size limit but also for next generation multistate 3D ReRAM.

Acknowledgment. This work was supported in part by SCOPE. The authors thank M. Kanai for constructive advice and T. Ishibashi for his invaluable technical support. T.K. and B.H.P. were partly supported by the WCU program through the NRF funded by MEST (Grant No. R31-2008-000-10057-0).

Supporting Information Available. Further experimental details, structural analysis, electrical measurements, and atmosphere-dependent data retention measurement. This material is available free of charge via the Internet at http://pubs.acs.org.

REFERENCES AND NOTES

(1) Pan, T.-M.; Yeh, W.-W. *Appl. Phys. Lett.* **2008**, *92*, 173506.
(2) Garcia, V.; Fusil, S.; Bouzehouane, K.; Enouz-Vedrenne, S.; Mathur, N. D.; Barthélémy, A.; Bibes, M. *Nature* **2009**, *460*, 81–84.
(3) Maruyama, T.; Shiota, Y.; Nozaki, T.; Ohta, K.; Toda, N.; Mizuguchi, M.; Tulapurkar, A. A.; Shinjo, T.; Shiraishi, M.; Mizukami, S.; Ando, Y.; Suzuki, Y. *Nat. Nanotechnol.* **2009**, *4*, 158–161.
(4) Lee, S.-H.; Jung, Y.; Agarwal, R. *Nat. Nanotechnol.* **2007**, *2*, 626–630.
(5) Jung, Y.; Lee, S.-H.; Jennings, A.-T.; Agarwal, R. *Nano Lett.* **2008**, *8*, 2056–2062.

DOI: 10.1021/nl9042906 | *Nano Lett.* **2010,** *10,* 1359–1363

(6) Lee, M.-J.; Han, S.; Jeon, S. H.; Park, B. H.; Kang, B. S.; Ahn, S.-E.; Kim, K. H.; Lee, C. B.; Kim, C. J.; Yoo, I.-K.; Seo, D. H.; Li, X.-S.; Park, J.-B.; Lee, J.-H.; Park, Y. *Nano Lett.* **2009**, *9*, 1476–1481.
(7) Ahn, S.-H.; Lee, M.-J.; Park, Y.; Kang, B. S.; Lee, C. B.; Kim, K. H.; Seo, S.; Suh, D.-S.; Kim, D.-C.; Hur, J.; Xianyu, W.; Stefanovich, G.; Yin, H.; Yoo, I.-K.; Lee, J.-H.; Park, J.-B.; Baek, I.-G.; Park, B. H. *Adv. Mater.* **2008**, *20*, 924–928.
(8) Yoshida, C.; Kinoshita, K.; Yamasaki, T.; Sugiyama, Y. *Appl. Phys. Lett.* **2008**, *93*, No. 042106.
(9) Choi, J.-S.; Kim, J.-S.; Hwang, I. R.; Hong, S. H.; Jeon, S. H.; Kang, S.-O.; Park, B. H.; Kim, D. C.; Lee, M. J.; Seo, S. *Appl. Phys. Lett.* **2009**, *95*, No. 022109.
(10) Chang, S.-H.; Lee, J. S.; Chae, S. C.; Lee, S. B.; Liu, C.; Kahng, B.; Kim, D.-W.; Noh, T. W. *Phys. Rev. Lett.* **2009**, *102*, No. 026801.
(11) Kim, K.-M.; Hwang, C.-S. *Appl. Phys. Lett.* **2009**, *94*, 122109.
(12) Rohde, C.; Choi, B. J.; Jeong, D. S.; Choi, S.; Zhao, J.-S.; Hwang, C. S. *Appl. Phys. Lett.* **2005**, *86*, 262907.
(13) Strukov, D.-B.; Snider, G.-S.; Stewart, D.-R.; Williams, R.-S. *Nature* **2008**, *453*, 80–83.
(14) Yang, J.-J.; Pickett, M. D.; Li, X.; Ohlberg, D. A. A.; Stewart, D. R.; Williams, R. S. *Nat. Nanotechnol.* **2008**, *3*, 429–433.
(15) Fujiwara, K.; Nemoto, T.; Rozenberg, M.-J.; Nakamura, Y.; Takagi, H. *J. Jpn. Appl. Phys.* **2008**, *47*, 6266–6271.
(16) Shima, H.; Takano, F.; Muramatsu, H.; Akinaga, H.; Tamai, Y.; Inque, I. H.; Takagi, H. *Appl. Phys. Lett.* **2008**, *93*, 113504.
(17) Shima, H.; Takano, F.; Tamai, Y.; Akinaga, H.; Inoue, I.-H. *J. Jpn. Appl. Phys.* **2007**, *46*, L57–L60.
(18) Nagashima, K.; Yanagida, T.; Oka, K.; Kawai, T. *Appl. Phys. Lett.* **2009**, *94*, 242902.
(19) Waser, R.; Aono, M. *Nat. Mater.* **2007**, *6*, 833–840.
(20) Szot, K.; Speier, W.; Bihlmayer, G.; Waser, R. *Nat. Mater.* **2006**, *5*, 312–320.
(21) Sawa, A. *Mater. Today* **2008**, *11*, 28–36.
(22) Kim, S.-I.; Lee, J.-H.; Chang, Y.-W.; Hwang, S.-S.; Yoo, K.-H. *Appl. Phys. Lett.* **2008**, *93*, No. 033503.
(23) Oka, K.; Yanagida, T.; Nagashima, K.; Tanaka, H.; Kawai, T. *J. Am. Chem. Soc.* **2009**, *131*, 3434–3435.
(24) Lu, W.; Lieber, C. M. *Nat. Mater.* **2007**, *6*, 841–850.
(25) Nagashima, K.; Yanagida, T.; Tanaka, H.; Seki, S.; Saeki, A.; Tagawa, S.; Kawai, T. *J. Am. Chem. Soc.* **2008**, *130*, 5378–5382.
(26) Oka, K.; Yanagida, T.; Nagashima, K.; Tanaka, H.; Seki, S.; Honsho, Y.; Ishimaru, M.; Hirata, A.; Kawai, T. *Appl. Phys. Lett.* **2009**, *95*, 133110.
(27) Marcu, A.; Yanagida, T.; Nagashima, K.; Oka, K.; Tanaka, H.; Kawai, T. *Appl. Phys. Lett.* **2008**, *92*, 173119.
(28) Yanagida, T.; Marcu, A.; Matsui, H.; Nagashima, K.; Oka, K.; Yokota, K.; Taniguchi, M.; Kawai, T. *J. Phys. Chem. C* **2008**, *112*, 18923–18926.
(29) Nagashima, K.; Yanagida, T.; Oka, K.; Tanaka, H.; Kawai, T. *Appl. Phys. Lett.* **2008**, *93*, 153103.
(30) Nagashima, K.; Yanagida, T.; Tanaka, H.; Kawai, T. *J. Appl. Phys.* **2007**, *101*, 124304.
(31) Marcu, A.; Yanagida, T.; Nagashima, K.; Tanaka, H.; Kawai, T. *J. Appl. Phys.* **2007**, *102*, 016102.
(32) Yanagida, T.; Nagashima, K.; Tanaka, H.; Kawai, T. *Appl. Phys. Lett.* **2007**, *91*, 061502.
(33) Nagashima, K.; Yanagida, T.; Tanaka, H.; Kawai, T. *Appl. Phys. Lett.* **2007**, *90*, 233103.
(34) Yanagida, T.; Nagashima, K.; Tanaka, H.; Kawai, T. *J. Appl. Phys.* **2008**, *104*, 016101.
(35) Nagashima, K.; Yanagida, T.; Klamchuen, A.; Kanai, M.; Oka, K.; Seki, S.; Kawai, T. *Appl. Phys. Lett.* **2010**, *96*, 073110.
(36) Klamchuen, A.; Yanagida, T.; Nagashima, K.; Seki, S.; Oka, K.; Taniguchi, M.; Kawai, T. *Appl. Phys. Lett.* **2009**, *95*, 053105.
(37) Constant, K.-P.; Mason, T.-O.; Rothman, S.-J.; Routbort, J.-L. *J. Phys. Chem. Solids* **1992**, *53*, 405–411.

DOI: 10.1021/nl9042906 | *Nano Lett.* **2010,** *10,* 1359–1363